Research Article | Vol. 26, No. 13 | 25 Jun 2018 | OPTICS EXPRESS 17662
Optics EXPRESS

Zadoff-Chu sequence-based upstream ranging in OFDMA-PON mobile radio access networks

AHMED GALIB REZA,[1] GEUN YOUNG KIM,[2] MYOUNG-SOO LEE,[3] AND JUNE-KOO KEVIN RHEE[1,*]

[1]KAIST, School of Electrical Engineering, 373-1 Guseong-dong, 305-701 Daejeon, South Korea
[2]HFR, Inc., Seongnam-daero 43beon-gil, Bundang-gu, 463-810 Gyeonggi-do, South Korea
[3]Crossworks, Inc., 18 Yeongdong-daero 129-gil, Gangnam-gu, Seoul, South Korea
*rhee.jk@kaist.edu

Abstract: Orthogonal frequency division multiple access (OFDMA) uplink in a passive optical network (PON) requires the delay alignment for OFDMA symbols from remotely distributed optical network units (ONUs). In this paper, we experimentally demonstrate and analyze the performance of a Zadoff-Chu (ZC) sequence-based upstream ranging scheme in an intensity modulation/direct detection (IM/DD)-based OFDMA-PON. The experimental results show that the proposed scheme can achieve upstream synchronization with only marginal inter-carrier interference (ICI) and requires no additional bandwidths in a typical OFDMA transmission with cyclic prefix (CP).

© 2018 Optical Society of America under the terms of the OSA Open Access Publishing Agreement

OCIS codes: (060.2330) Fiber optics communications; (060.4080) Modulation.

References and links

1. T. O. Olwal, K. Djouani, and A. M. Kurien, "A survey of resource management toward 5G radio access networks," IEEE Commun. Surv. Tutorials **18**(3), 1656–1686 (2016).
2. A. Yazdan, J. Park, S. Park, T. A. Khan, and R. W. Heath, "Energy-efficient massive MIMO: wireless-powered communication, multiuser MIMO with hybrid precoding, and cloud radio access network with variable-resolution ADCs," IEEE Microw. Mag. **18**(5), 18–30 (2017).
3. C. Mobile, "C-RAN: the road towards green RAN," White paper V 2.5 (2011).
4. Common public radio interface (CPRI); interface specification, CPRI specification V 6.1, Ericsson AB, Huawei Technologies Co. Ltd, NEC Corporation, Alcatel Lucent, and Nokia Networks, http://www.cpri.info (2014).
5. K. Kanonakis, I. Tomkos, T. Pfeiffer, J. Prat, and P. Kourtessis, "ACCORDANCE: A novel OFDMA-PON paradigm for ultra-high capacity converged wireline-wireless access networks," in *Proceedings of International Conference on Transparent Optical Networks* (ICTON, 2010), pp. 1–4.
6. J. von Hoyningen-Huene, H. Griesser, M. Eiselt, and W. Rosenkranz, "Asynchronous signal reception in OFDMA-PON-uplink," in *Advanced Photonics* 2013, paper SPM4D.2.
7. J. von Hoyningen-Huene, H. Griesser, M. H. Eiselt, C. Ruprecht, and W. Rosenkranz, "Comparison of Rx-DSP-structures in experimental OFDMA-PON uplink transmission systems," in *Proceedings of Optical Fiber Communication Conference* (OFC, 2014), paper Tu2F.4.
8. S. Y. Jung, S. M. Jung, H. J. Park, and S. K. Han, "Mitigation of timing offset effect in IM/DD based OFDMA-PON uplink multiple access," Opt. Express **23**(11), 13889–13898 (2015).
9. X. Peng, J. Chen, Y. Li, and Y. Song, "Single subcarrier gold sequences modulated timing synchronization for upstream OFDMA-PON," IEEE Photonics J. **9**(1), 7200207 (2017).
10. A. Razmtouz, K. Habel, C. Kottke, C. Ruprecht, and W. Rosenkranz, "Initial ranging scheme based on interpolated Zadoff-Chu sequences for OFDMA-PON," Opt. Express **22**(3), 3669–3674 (2014).
11. B. Kuang and Y. Wu, "Ranging timing synchronization for OFDMA-PON upstream," in *Proceedings of Asia Communications and Photonics Conference* (ACP, 2014), paper ATh3A.177.
12. A. G. Reza and J.-K. K. Rhee, "Zadoff–Chu sequence-based hitless ranging scheme for OFDMA-PON configured 5G fronthaul uplinks," Opt. Eng. **56**(5), 056110 (2017).
13. R. L. Frank, S. A. Zadoff, and R. Heimiller, "Phase shift pulse codes with good periodic correlation properties," IRE Trans. Inf. Theory **IT-8**(6), 381–382 (1962).
14. D. C. Chu, "Polyphase codes with good periodic correlation properties," IEEE Trans. Inf. Theory **18**(4), 531–532 (1972).
15. Telesystem Innovations Inc, white paper, "LTE in a nutshell: the physical layer," (Telesystem Innovations Inc., 2010), http://frankrayal.com/wp-content/uploads/2017/02/LTE-in-a-Nutshell-System-Overview.pdf.

#325446 https://doi.org/10.1364/OE.26.017662
Journal © 2018 Received 9 Mar 2018; revised 3 Jun 2018; accepted 8 Jun 2018; published 22 Jun 2018

Optics EXPRESS

1. Introduction

The next-generation 5G radio access networks (RANs) are anticipated to facilitate a seamless ubiquitous connectivity and to provision billions of mobile devices with 1000-fold more Internet data traffic, which entails a higher bandwidth and quality of service (QoS) requirements than Long Term Evolution (LTE) by 2020 [1]. To meet such high requirements, massive MIMO (multiple-input multiple-output) is often considered as a primary candidate in which hundreds of MIMO antennas are typically integrated into base stations (BSs), which is envisioned as a stand-alone object [2]. One of the major technical challenges due to such densifications of cellular networks are inter-cell interference, increased capital expenditure (CAPEX) and operational expenditure (OPEX). Cloud RAN (C-RAN) [3] is a new type of RAN architecture that offers a centralized baseband processing, in which a number of remote radio heads (RRHs) are connected to a centralized baseband unit (BBU) pool using the common public radio interface (CPRI) [4]. CPRI is the major limiting factor of today's C-RAN technology as it is often configured in a point-to-point fashion that transports uncompressed digital IQ samples, requiring a very large bandwidth. If the CPRI data transmission can be realized using a splitter-based direct-detection OFDMA-PON technology then a point-to-multipoint (P2mP) connection can be established by employing only low-cost and fewer electronic components, as it can alleviate the requirement for a complex and costly tunable optical filter [5]. However, there are two major limiting factors for the realization of CPRI transmission using the present direct-detection OFDMA-PON technology in the uplink: (1) optical beating interference (OBI), and (2) OFDMA symbol timing offset due to asynchronous uplink transmission that causes both ICI and inter-symbol interference (ISI) at the receiver of an optical line terminal (OLT).

In this paper, our major focus is on the symbol timing offset problem, which can significantly increase the size, cost, and complexity of the PON system. One of the techniques to mitigate symbol timing offset is to employ multiple fast Fourier transforms (FFT) and DSP blocks at the OLT-side, dedicated to each ONU to separately process each asynchronous uplink OFDMA signal [6-7]. It can only mitigate demodulation failure problems, while leaving the ICI problems unresolved. Another simple timing offset mitigation technique to synchronize OFDMA symbol phase is to extend the CP in an OFDMA symbol boundary [8], which requires an additional bandwidth. When the arrival timing offset from a newly joining ONU is greater than the range of a CP, the ICI penalties will occur on the subcarriers that are already in service. In this regard, a preamble-based timing offset estimation technique can be a very practicable solution. However, this process is often incompatible with the use of the CP that can cause an ICI while the symbol time position is incorrect, or requires a guardband and dedicated ranging carriers in the spectrum [9–11].

Recently, we have proposed a hitless upstream ranging scheme using ZC sequences under a gradual loading condition for a direct-detection OFDMA-PON system for mobile fronthaul applications, which can avoid guardbands in the spectrum [12]. In this scheme, phase continuity over each CP is achieved by a frequency-domain phase precoding at the ONU, which results in a gradual slip of the autocorrelation-peak position with respect to an OFDMA symbol with CP. The gradual loading scheme enables the receiver to detect only one auto-correlation peak with the highest magnitude. In this paper, we experimentally verify the performance of the proposed hitless upstream ranging scheme by introducing optical path differences between two ONUs up to 18-km, which absolutely falls beyond the CP tolerance bound. After 20-km transmission over a standard single mode fiber (SSMF) for two concurrent asynchronous ONUs at an aggregated data rate of 11.5 Gbps, the system performance in terms of error vector magnitude (EVM) confirms that the proposed scheme can achieve upstream synchronization with requiring no additional bandwidths.

Optics EXPRESS

2. Hitless upstream ranging scheme

In an OFDMA-PON system, the symbols received from each ONU must fit within an FFT window at the OLT for an interference-free transmission, as shown in Fig. 1(a). Due to asynchronous nature of the OFDMA-PON upstream transmission scheme, the symbols from different ONUs may not fit within a single OLT FFT window [Fig. 1(b)], if the time delay is longer than the length of the CP, which is formed due to an arbitrary length of distribution fibers. It can generate a significant amount of crosstalk and can break orthogonality between OFDMA subcarriers.

In our work, a ZC [13-14] sequence, which is a subset of CAZAC sequences, is used for the ranging process. The ONU who wants to join the network transmits the ZC sequences, which are autocorrelated in the OLT, and the location of the autocorrelation peak position is used to find the timing offset. The major motivation behind the proposition of using a ZC sequence is its sharp autocorrelation peaks and zero sidelobes. To generate such a ZC sequence, an inverse Fourier transform of the following Fourier sequence can be used:

$$C(k)=\begin{cases}\exp\left(-j\pi r\dfrac{k^2}{L}\right), & \text{for even } L,\\ \exp\left(-j\pi r\dfrac{k(k+1)}{L}\right), & \text{for odd } L,\end{cases} \tag{1}$$

where L denotes the length of the ZC sequence, r is relatively prime to L representing a root sequence index, and $k = 0, 1,\ldots, L\text{-}1$ is the index for frequency component, or the subcarrier.

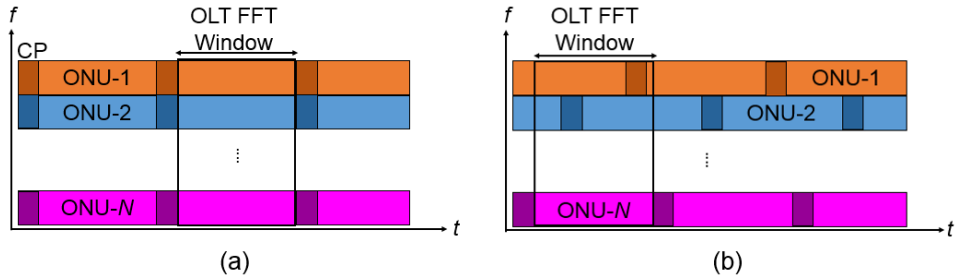

Fig. 1. Signal reception in the OFDMA-PON uplink. (a) Synchronous transmission. (b) Asynchronous transmission.

However, when a ranging ONU transmits ranging symbols asynchronously, abrupt changes or discontinuities due to a sudden change of subcarrier modulations or CP attachments in the time domain can cause an inter-carrier leakage of a substantial amount of energy in the frequency domain, which introduces a non-negligible amount of ICI to the other subcarriers already in service. In order to avoid such a sudden change of subcarrier modulations, we consider a gradual loading of the ZC sequences such that the magnitudes of the autocorrelation peaks vary with the number of ZC sequences loaded on the assigned OFDMA subcarriers. In order to generate such an effect, the following ZC loading model is considered:

$$X(k,t)=\begin{cases}C(k), & \text{if } 1\le k\le\dfrac{(t-1)D}{2} \text{ or } L-\dfrac{(t-1)D}{2}+1\le k\le L\\ 0, & \text{otherwise}\end{cases} \quad \begin{matrix}t=1,\ldots,N_T/2+1\\ k=1,2,\ldots L\end{matrix}, \tag{2}$$

where $X(k,t)$ denotes a gradual loading of the ZC sequences as a function of relative subcarrier index k with respect to the first subcarrier of the ranging ONU at symbol index t in the time domain (e.g., t = 1 corresponds to the first symbol in the ranging sequence), L

Optics EXPRESS

denotes the allocated number of subcarriers to the ranging ONU, D represents the number of carriers loaded with a ZC sequence, and N_T represents the period of autocorrelation peak modulation. Once the ZC sequences are loaded on all subcarriers, the ranging ONU will gradually unload to its initial value (zero) in the reverse order.

If we assume that only L OFDMA subcarriers are allocated to the ranging ONU among K available subcarriers in the entire upstream spectrum, then the ranging ONU can load the ZC sequences generated in Eq. (2) to its assigned spectrum as

$$\tilde{X}(n,t)=\begin{cases} X(n-m+1,t), & \text{for } m\le n\le m-1+L,\\ 0, & \text{otherwise,}\end{cases} \quad \text{for } n=0,1,\ldots,K\text{-}1, \qquad (3)$$

where m is the index of first subcarrier among L assigned subcarriers to the ranging ONU.

In the process of CP attachment, the ranging signals can produce discontinuities on the boundaries between OFDMA symbols, which can cause an ICI if the OFDMA symbol is off aligned. The blue curve in Fig. 2 shows a discontinuity in one of the ranging subcarriers due to a CP attachment. From the figure, we can also notice a sudden change of phase on the boundary of the OFDMA symbols. The phase precoding is intended to remove such a discontinuity, as shown with the red curve in Fig. 2, using the following equation:

$$\tilde{X}'(n,t)=\tilde{X}(n,t)e^{j2\pi n(t-1)\frac{N_{CP}}{2K}}, \qquad (4)$$

where N_{cp} is the length of CP. Here, we impose a Hermitian symmetry in the OFDMA systems as an example, where $2K$ denotes the IFFT size for K service subcarriers. The Hermitian symmetry is attained by $X_{2K-n} = X^*_n$, where $n = 0,1,\ldots, K\text{-}1$. However, this introduces a gradual slip of the autocorrelation peak position by the CP length for every ranging symbol as the precoding cumulates phase compensation over a sequence of ranging symbols. In order to mark a certain peak for synchronization, we use the property of gradual loading, with which the autocorrelation peak intensity changes with the cumulated amount of slips, according to our ranging signal design given in Eq. (2) and Eq. (4). This will allow the receiver to detect only one autocorrelation peak with the maximum magnitude to measure the OFDMA symbol offset deterministically.

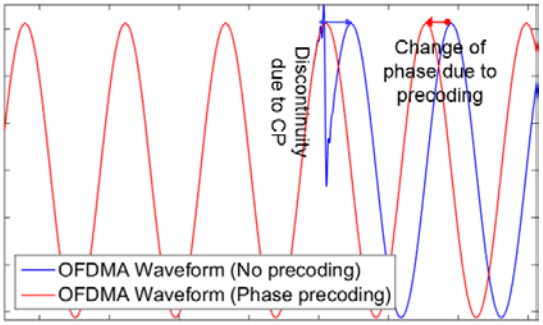

Fig. 2. Discontinuity mitigation in a time domain OFDMA symbol by a phase precoder.

Now, the OLT will use a complete set of ranging sequence to find the autocorrelation between the received signal $r(i)$ and the ranging code $seq(i+\tau)$ as

$$\hat{r}_{rseq}(\tau)=\sum_{i=0}^{2K+N_{cp}-1} r(i)*seq(i+\tau) \qquad (5)$$

Optics EXPRESS

The OLT will calculate $\hat{r}_{rseq}(\tau)$ over N_T number of OFDMA symbols. Next, the relative time delay can be found as $\hat{d}(\mathrm{n}) = \arg\max_{n}\{\| \hat{r}_{rseq}(\tau) \|\}$ by accepting only one autocorrelation peak with the highest magnitude. Now, the OLT will send a response message with adjustment parameters to the ranging ONU to tune the transmitter symbol clock phase. Subsequently, after removing the CP and S/P conversion, a 2*K*-point FFT is performed to decode the data of the synchronized ONUs with no ICI. This process may fail when two or more ONUs are added simultaneously, which may happen very rarely in the field applications.

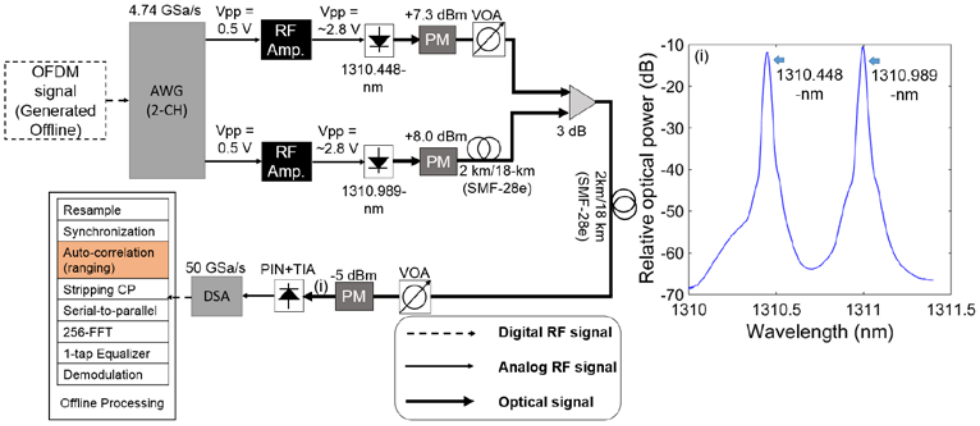

Fig. 3. Experimental setup of the proposed ZC sequence-based uplink synchronization scheme. (i) optical spectrum after 20-km transmission over SMF-28e.

3. Experimental setup

The schematic of the experimental setup is illustrated in Fig. 3, in which the entire OFDMA spectrum is assumed to be shared between two ONUs. A two-channel arbitrary waveform generator (Tektronix AWG 70002A) is used to produce a baseband OFDMA signal, generated offline with MATLAB using a 256-IFFT with a CP length of 6.25%. According to the LTE specification, the length of a normal CP is limited to 7.5% [15]. In our system, we chose the length of the CP to be 16 over an OFDMA symbol with a length of 256. The subcarrier spacing is 17.408 MHz (15.36*17/15), which can be synchronized to the 10MHz LTE sampling rate of 15.36 MHz with a channel overhead. The OFDMA signals are modulated with a 64-QAM modulation format. The peak-to-peak voltage (*Vpp*) of each AWG output is 0.5V, which is fed to an RF-attenuator before being amplified by a linear RF-amplifier. The resulting ~2.8V (*Vpp*) analog signals are modulated onto optical carriers using directly modulated lasers (Optilab DFB-1310-DM-10), with optical powers of + 8.0 dBm and + 7.3 dBm, respectively. We consider a general model of an OFDMA-PON, where uplink lasers can accept any arbitrary wavelength unless the wavelength coincides to each other in order to avoid OBI. In our analysis, the OBI penalty can be mitigated if the wavelengths are separated far enough compared with the OFDMA bandwidth. When the wavelengths from different ONUs are too close to each other, the OBI penalty should be resolved by tuning the wavelengths of the ONUs through controlling the temperature or current of the laser diode. Although this scheme can limit the scalability of an OFDMA-PON system, we consider the application of this scheme in the mobile radio access networks, where the number of ONUs are relatively small. In our experiment, a wavelength separation of ~0.54nm [Fig. 3(i)] is realized by letting the two ONUs to respectively transmit on 1310.989-nm and 1310.448-nm wavelengths to suppress any OBIs in the desired electrical passband. Due to zero dispersion at 1310-nm transmission, the frequency chirping is not a critical issue. For IM/DD detection, a Hermitian symmetry is obtained, which offers a net bit rate of 11,489.280 Mbps (110

Optics EXPRESS

subcarriers). For asynchronous uplink transmission, optical path differences between two ONUs are set to two and eighteen kilometers. A variable optical attenuator (VOA) is placed at an ONU to ensure that the received optical powers from the two ONUs at the remote node (RN) are comparable. After multiplexing at the RN by a 3dB passive optical coupler, the combined optical signals are launched onto two and eighteen kilometers feeder fibers, with an attenuation of 0.33 dB/km. Although two ONUs are used in transmission, a VOA is utilized in the system to emulate a higher fan-out loss at a PON splitter with higher ONU counts.

At the OLT, the received optical signals (maintained –5dBm) are detected by a 10 GHz linear InGaAs PIN + TIA (DSC-R402PIN) for optical-to-electrical conversions and then sampled by a real-time digital serial analyzer (Tektronix DSA 72004) at 50 GSa/s. Finally, the captured samples are processed offline in MATLAB for performance evaluation.

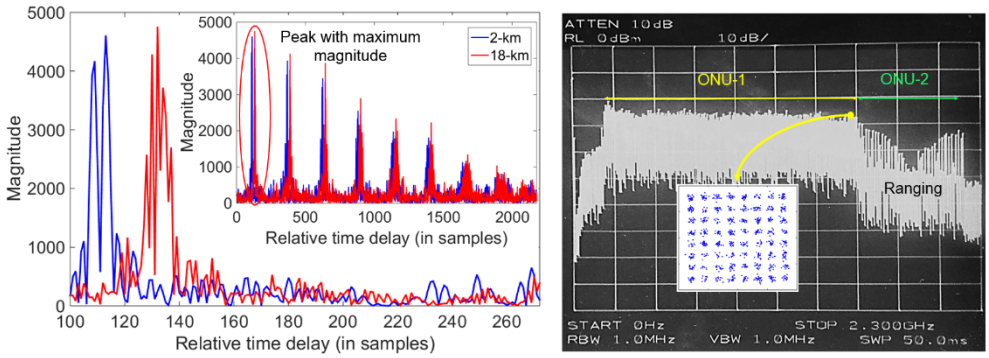

Fig. 4. (a) The highest peaks of the auto-correlations for 2-km and 18-km optical path delays. (b) Received RF spectra at the OLT during ranging.

4. Results

Figure 4(a) shows the highest peaks of the auto-correlation results for different optical paths from which the relative timing offsets between two ONUs are estimated at the OLT in the unit of sample positions in an OFDMA symbol, which consists of 272 samples including 16 for CPs. The optical path differences between two ONUs are set to 2-km and 18-km, and their corresponding auto-correlation results are shown in blue and red curves. In the inset, a gradual decrease of the auto-correlation peaks are observed as we decrease the number of subcarriers modulated with the ZC sequences. In this way, only one auto-correlation peak with the maximum magnitude can be detected. The detected RF spectra is shown in Fig. 4(b), where ONU-1 is already in service with a group of subcarriers indexed from 11 to 88, and ONU-2 is in ranging process and transmitting the ZC sequences onto a group of subcarriers from 89 to 120. In a typical system, the RF circuitry avoids DC coupling that can cause problems in the transmission. Hence, in our experimental design, we applied AC coupling with a low pass cut-off of ~300 MHz, which limits the use of low frequency OFDMA subcarriers indexed from 1 to 10. In this experiment, we chose D = 4 as discontinuity parameter, which was optimized in [12]. In the inset of Fig. 4(b), the constellation of the edge subcarrier (SC-88) is shown, which produces the worst EVM performance of 6.20% during the ranging process. It falls within the 3GPP requirements for 64-QAM, which confirms that the proposed scheme can achieve upstream synchronization without requiring any guard bands in the spectrum.

For comparisons, the EVM performances during asynchronous OFDMA-PON upstream transmissions are illustrated in Fig. 5 under different scenarios in terms of subcarrier assignments and optical path delay. The received constellations are shown in the insets. In the experiment, four different subcarrier allocation plans are considered: Case-1: ONU-1: 11-56 (46 carriers) and ONU-2: 57-120 (64 carriers), Case-2: ONU-1: 11-42 (32 carriers) and ONU-

Optics EXPRESS

2: 43-74 (32 carriers), Case-3: ONU-1: 11-24 (14 carriers) and ONU-2: 25-120 (96 carriers), and Case-4: ONU-1: 11-88 (78 carriers) and ONU-2: 89-120 (32 carriers). In Fig. 5(a) and Fig. 5(b), the optical path delays between ONU-1 and ONU-2 are set to 2-km and 18-km, respectively. To achieve a comparable performance, the received relative per subcarrier RF power is adjusted to −25 dBm in all four cases. From the figure, we can see that the EVM performances in all four cases are nearly identical for both ranging and synchronous data transmissions, which confirm that the proposed ZC ranging sequence does not interfere with the subcarriers that are already synchronized and in service. In addition, subcarrier-wise EVM performance nearly remains flat over the whole OFDMA spectrum with a marginal discrepancy in performance at the edge carrier due to a tolerable ICI formed during the ranging process, which can be easily fixed with bit-loading or by skipping one subcarrier while loading the ZC sequences to the ranging ONU. Finally, the EVM performances for both 2-km and 18-km optical path delays are comparable and below 8% (3GPP requirement for 64-QAM).

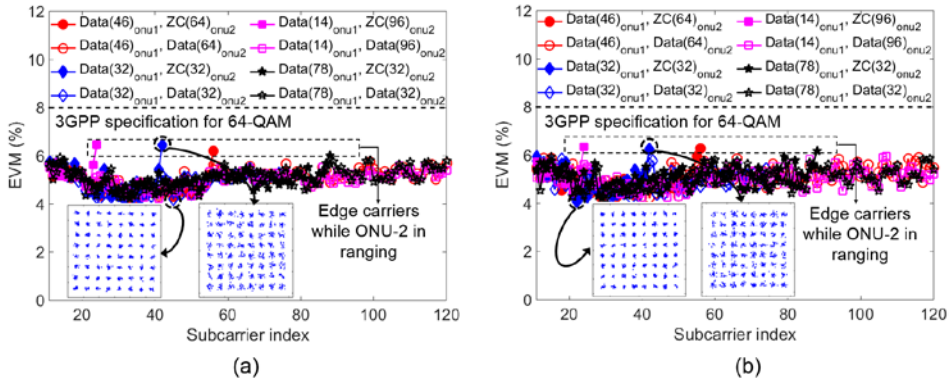

Fig. 5. EVM plots and constellations during asynchronous OFDMA-PON upstream signal transmission. (a) 2-km optical path delay, (b) 18-km optical path delay.

5. Conclusion

In this work, we experimentally demonstrated a realistic uplink transmission scheme in an OFDMA-PON system that allows the gradual hitless addition of new ONUs. In an OFDMA-PON system, a small timing offset could lead to a critical interference. In the experiment, two ONUs that are simultaneously transmitting symbols to an OLT via different lengths of optical fibers are used to demonstrate a seamless addition of a new ONU. The OFDMA system used Hermitian symmetry to realize IM/DD OFDMA symbols. The experimental results for EVM performances in an OFDMA-PON with the aggregated throughput of 11.5 Gbps confirm that the proposed ZC sequence-based upstream ranging scheme can successfully achieve upstream synchronization without producing any significant ICI to the in-service OFDMA carriers.

Funding

ICT R&D program of MSIP/IITP (1711057505, Reliable crypto-system standards and core technology development for secure quantum key distribution network); BK21 program of the School of Electrical Engineering, KAIST.